Research Paper

日本冷凍空調学会論文集
Trans. of the JSRAE
Vol○○, No.○ (2008)
原稿受付：○○○○年○月○日

Investigating the Contribution of Urban Canopy Model and Anthropogenic Heat Emission to Urban Heat Island Effect using WRF Model

Kundan Lal SHRESTHA *† Akira KONDO * Chikara MAEDA *
Akikazu KAGA * Yoshio INOUE *

* Division of Sustainable Energy and Environmental Engineering, Osaka University
(2-1 Yamadaoka, Suita-shi, Osaka 565-0871)

Summary

Heat island effect changes the local weather pattern, increases energy costs to offset this effect, and also increases demand for cooling. While considering urban heat island, local effects due to waste heat from anthropogenic emissions from vehicles should also be taken into consideration. In this research, state-of-the-art WRF model coupled with urban canopy model has been modified by including the gridded anthropogenic heat emission data of Osaka, Japan for meteorological modeling of Osaka region in order to assess the contribution of urban canopy effect and anthropogenic heat emission towards the formation of urban heat island. We developed and used a detailed urban land-use map to be used for urban canopy modeling, and a gridded emission map consisting of spatial and seasonal distribution of anthropogenic heat emission for better representation of urban heat emission. Using area-averaged and one-week averaged time series simulation results, we could understand the spatial and temporal behavior of urban heat island effect in more detail. The results showed an average increase of 0.8 K in near-surface air temperature in Osaka City when anthropogenic heat and urban canopy effect were taken into consideration.

Key words: Urban heat island, Anthropogenic heat, Simulation, Urban canopy model, WRF model

1. Introduction

The effect of urbanization on the regional and local scale climate is well-known, and urban warming, or urban heat island effect, is one of the major consequences of urban development. Urban warming in a regional setting with complex land-use including green space and suburban vegetation is caused by a blend of different physical factors such as the so-called urban canopies, surface materials and their characteristics, moisture characteristics, anthropogenic heat flux, and air pollution. Urban warming increases demand for air conditioning, and consequently, more air conditioners generate more heat and adversely affect the local scale climate including human comfort and demand for cooling [1]. Thus the understanding of the causes of urban heat island effect is crucial in developing and implementing mitigation strategies for urban warming.

Though WRF (Weather Research and Forecasting) model is good at predicting daytime air temperature,

†Fax: +81 6-6879-7670 E-mail: kundan@ea.see.eng.osaka-u.ac.jp

it has a tendency to underestimate urban nocturnal air temperature [2]. This can adversely affect the simulation of nocturnal heat island. To add the contribution of heat from urban canopy, WRF is coupled with an urban canopy model. The use of urban canopy model in idealized experiments with two-dimensional atmospheric model has shown the importance of using urban canopy models for the nocturnal heat island [3,4]. Nocturnal heat island is caused by the larger heat storage of the canopy model, which gets released as sensible heat at nighttime [3]. Sensitivity experiments in idealized conditions have revealed that anthropogenic heating has a greater impact on the nocturnal temperature than other urban canopy parameters like heat capacity of wall, sky view factor and albedo [4].

Though experiments related to urban heat island have been generally carried out for the Tokyo region in Japan [5], such experiments are scarcely available for Osaka, which is one of the metropolitan cities of Japan.

This research investigates the urban heat island phenomenon in Osaka (see Fig. 1 for terrain structure of the area used in this research), using real meteorological conditions in WRF model. To impart a realistic modeling approach to the investigation of the effects of urban canopies and anthropogenic heat flux in an urban setting, WRF mesoscale model, coupled with an urban canopy model, was modified to accommodate the gridded hourly anthropogenic heat flux data. Compared to the idealized experiments, the use of real meteorological conditions in a mesoscale model can improve the accuracy and authenticity of the simulation results.

The spatial and temporal development of urban heat island is complicated by the complex distribution of urban structure and anthropogenic heat emission at local and urban scales. Diurnal anthropogenic heating profiles have been used in mesoscale models to use anthropogenic heat flux as a heat source, which is evenly-distributed in the surface layer [6,7]. Though previous findings have pointed out the improvement in urban heat island simulation using only the area-averaged anthropogenic heat and land-use parameters in a meteorological model, this research uses gridded high-resolution urban land use data and hourly gridded anthropogenic heat map of Osaka to validate the importance of anthropogenic heat and urban canopy model in the heat island phenomenon in Osaka.

2. Model Data and Description

2.1 WRF Model

WRF model is a numerical weather prediction and atmospheric simulation system with a flexible, modular and portable code design, and it is also regarded as a successor to the widely used MM5 model [8].

UCM (Urban Canopy Model) used in WRF is a single-layer canopy model for energy and momentum exchange between the urban surface and the atmosphere, which includes the influence of street canyons, shadowing from buildings and reflection of radiation, anthropogenic heating, and multi-layer heat transfer equation for roof, building wall and road surfaces [9]. Since it includes canyon orientation and the diurnal variation of solar azimuth angle, it can represent more realistic geometry than the commonly used slab models in meteorological models. This urban canopy model is coupled with the unified Noah land surface model used in the WRF modeling system.

2.2 Developing urban land-use data

In urban canopy model of WRF, the urban land-use has to be sub-categorized according to various parameters like building height, building coverage and urban fraction in each grid cell. For this, we divided the urban category into three sub-categories, viz., high-density residential, medium-density residential, and low-density residential (Fig. 2).

1997's 100-m National Digital Information data were used to obtain the 1-km land-use distribution for other non-urban land use categories.

Detailed Digital Information (10-m Grid Land Use) data obtained from Japan Map Center for the Kinki region were used to create a detailed urban

land-use map needed for urban canopy model.

Average building height and building coverage data are available in Osaka City Mesh Data. To obtain building height data for urban canopy model, the building height data from Osaka City Mesh Data were associated with the 10-m grid urban land-use data from Detailed Digital Information. From this data, the building height was calculated at each of the 1-km grid cells by averaging the height of the buildings falling on those grid cells.

2.3 Urban canopy model parameters

The important parameters of the urban canopy model are selected for the model region so that they reflect the actual urban canopy structure and properties (Table 1). Urban fraction was calculated as

$$FRC\_URB = A_{URBAN} / A_{GRID} \quad (1)$$

where,

A_{URBAN}: area covered by urban region

A_{GRID}: area of the whole grid.

Building coverage ratio is calculated as

$$R = A_{BUILDING} / A_{URBAN} \quad (2)$$

where,

$A_{BUILDING}$: area covered by the buildings in the grid.

In this simulation study, we have sub-categorized the urban land-use according to the urban fraction of each grid cell. As can be inferred from Table 1, the sub-categorization using building height is not worthwhile in the case of Osaka region due to small differences in building heights among the different urban types. So we have sub-categorized urban land-use category according to the evenly distributed urban fraction data.

The grid-scale flux for urban grid fraction is calculated by urban canopy model and the rest of the non-urban fraction is calculated by Noah land surface model of WRF. Then the total flux is calculated as

$$F = FRC\_URB * F_{URBAN} + (1\text{-}FRC\_URB) * F_{NON\text{-}URBAN} \quad (3)$$

where,

F: total flux

F_{URBAN}: flux calculated by urban canopy model

$F_{NON\text{-}URBAN}$: flux calculated by Noah land surface model.

Table 1 Important parameters of urban canopy model depending on land-use category

Name	Unit	Low-density residential	Medium-density residential	High-density residential
Building height	m	7.5	8.1	8.2
Building coverage ratio	-	0.46	0.49	0.50
Urban fraction	-	0.52	0.79	0.92

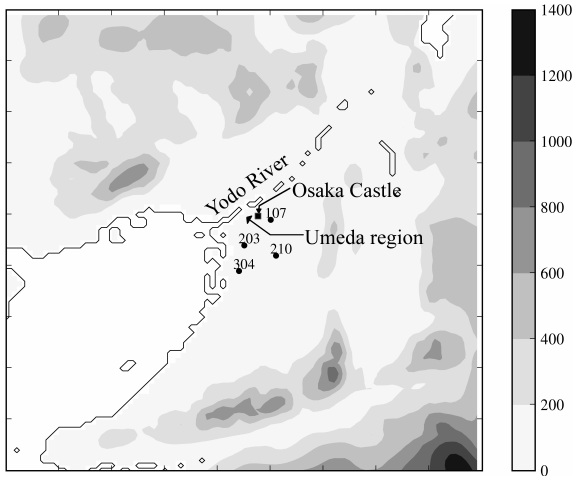

Fig. 1 Terrain height (in meter) of the model region. 107, 203, 210 and 304 (see Table 4) are the observation stations used for comparison with the model results. The shown region is the same region as Domain-2 in Fig. 4.

2.4 Anthropogenic heat flux

The hourly anthropogenic data in 1-km grids for the Kinki region are available [10] (see Fig. 3 for a typical example of gridded anthropogenic heat flux data used in the model region). The yearly average of anthropogenic heat fluxes from vehicle and railroads is used in the present study. Similarly, August average of anthropogenic heat flux from the release of waste heat from building and commercial energy consumption and human metabolism is used.

There are sensible and latent anthropogenic heat fluxes available that are separately processed and ingested in the WRF model.

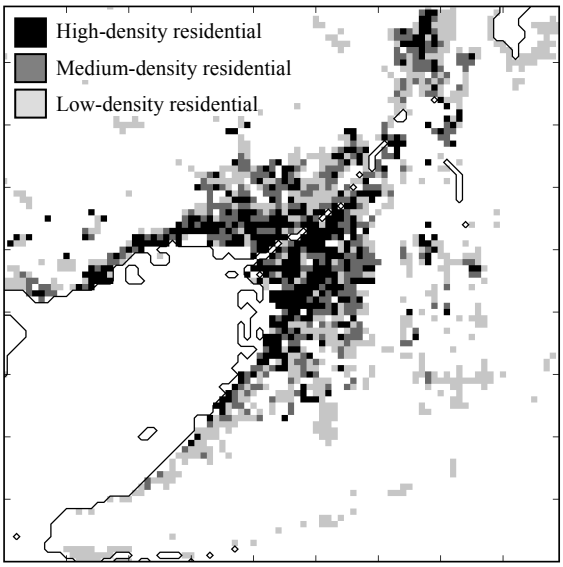

Fig. 2 Sub-categories of urban land-use in model region. The shown region is the same region as Domain-2 in Fig. 4.

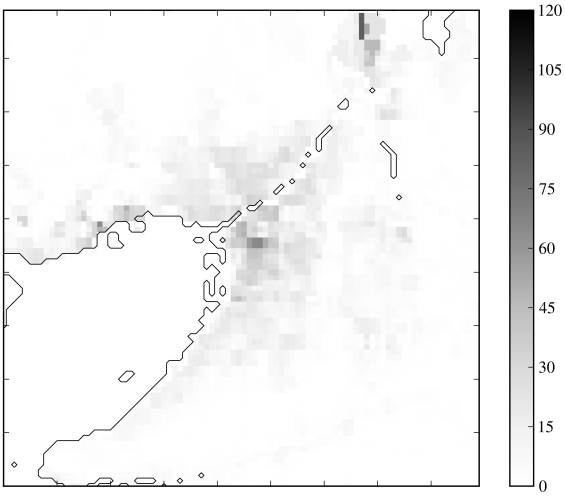

Fig. 3 Sensible anthropogenic heat flux (W/m^2) at 2000 JST. The shown region is the same region as Domain-2 in Fig. 4.

The gridded anthropogenic data are interpolated to the WRF grid structure by a preprocessing program called WPS (WRF Preprocessing System).

3. Simulation method

3.1 Meteorological modeling using WRF

Parameters and schemes shown in Table 2 were used to run the WRF model in a 1-km gridded domain nested inside a 3-km gridded domain (Fig.3). Vertical grid structure was configured with 24 terrain-following eta levels. The topmost level was set at 100 hPa and the thickness of the first and second levels from the land surface were about 25 and 65 meters respectively.

The initial conditions for the WRF grid were obtained by preprocessing the high-resolution GPV-MSM (Grid Point Value – Mesoscale Model) meteorological data on 0.1x0.125 degree Japanese grids (for pressure levels) obtained from Japan Meteorological Agency.

Table 2 Important WRF parameters and schemes

Parameter/scheme	Model setting
Land surface	Noah land surface model
Cumulus	None
Radiation	RRTM
Microphysics	WSM 3-class
PBL scheme	YSU
Domains	3-km and 1-km grids
Nesting	One-way
Time period	August 8-14, 2007

Soil moisture and temperature below ground level required for the Noah land surface model were obtained from the FNL (Final) Global Analyses on 1.0x1.0 degree global grids provided by NCEP (National Centers for Environmental Prediction).

One-way nesting was utilized to solely observe the effect of using anthropogenic heat and urban canopy model in the 1-km grid. The boundary conditions for the 1-km grid are provided by the larger mother domain having 3-km grid structure (Fig. 4).

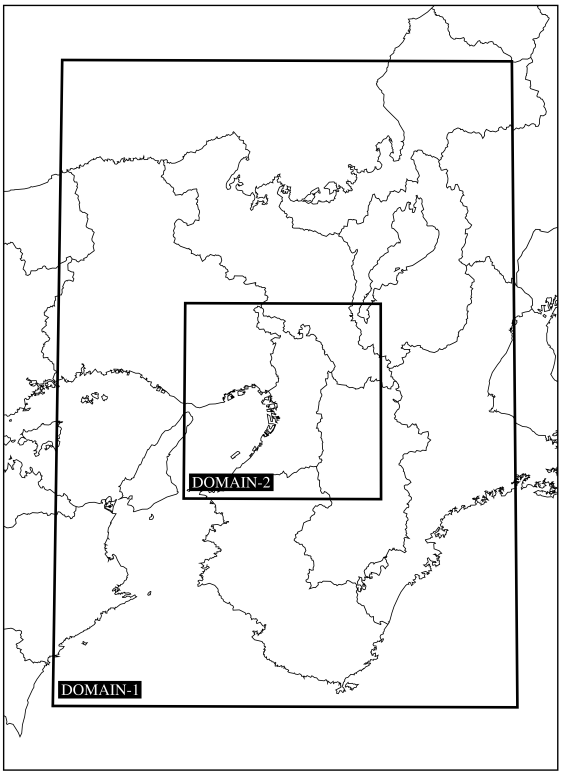

Fig. 4 Domain configuration used in WRF simulation. Domain-1 is the mother domain having 3-km grid structure. Domain-2 is the nested domain having 1-km grid structure, which also contains the Osaka region.

3.2 Modification in PBL scheme

For summer, the anthropogenic heat mainly reflects the release of waste heat from building and commercial energy consumption and human metabolism, and thus, it is directly vented into the atmosphere. So it may be directly introduced into the thermodynamic equation as an additional source term at the first level above ground [6].

Though urban canopy model in WRF contains a simple diurnal representation of anthropogenic heat emission, we have disabled this feature because it cannot represent the actual spatio-temporal emission pattern of anthropogenic heat. So we have used an explicit representation of hourly gridded anthropogenic heat data in the PBL scheme.

YSU (Yonsei University) PBL scheme [11] in the WRF model is the next generation of the MRF PBL commonly used in MM5 model, and it uses an explicit treatment of the entrainment layer at the PBL top in addition to countergradient terms to represent fluxes due to non-local gradients. YSU PBL scheme is modified in order to include anthropogenic heat as an additional source term at the first level above ground. Eq. (4) is the thermodynamic equation based on YSU PBL scheme.

$$\frac{\partial C}{\partial t}=\frac{\partial}{\partial z}\left[K_c\left(\frac{\partial C}{\partial z}-\gamma_c\right)-(\overline{w'C'})_h\left(\frac{z}{h}\right)^3\right] \tag{4}$$

where,

C: θ, q

θ: potential temperature

q: mixing ratio for water vapor, cloud, ice

z: height from the surface

h: height of boundary layer

K_c: exchange coefficient

$(\overline{w'C'})_h$: flux at the inversion layer

$(\overline{w'C'})_h(z/h)^3$: asymptotic entrainment flux term at the inversion layer

γ_c : $b\dfrac{(\overline{w'C'})_O}{w_{so}h}$ (correction to the local gradient that incorporates the contribution of the large-scale eddies to the total flux)

b: 6.8 (coefficient of proportionality)

$(\overline{w'C'})_O$: surface flux

w_{so} : mixed-layer velocity scale at z=0.5h

In the numerical formulation of potential temperature equation, the equation for the bottom layer (layer 1) is given as

$$(1+\delta_1)\theta_1^{n+1}-\delta_1\theta_2^{n+1}=\theta_1^{n-1}+\delta_1\mu_1+\beta \tag{5}$$

where,

$\delta_k=\dfrac{2\Delta t\,K_{k-1}}{\Delta\hat{z}_{k-1}\Delta\bar{z}_k}$

$\Delta\hat{z}_k$: distance between θ_{k+1} and θ_k

$\Delta\bar{z}_k$: distance between $\bar{\theta}_{k+1}$ and $\bar{\theta}_k$

$\mu_k=\alpha\Delta\hat{z}_k$

$\alpha=-\gamma-(\overline{w'\theta'})_h\left(\dfrac{z}{h}\right)^3K^{-1}$

$\beta=\dfrac{2\Delta t\,H_0}{\Delta\bar{z}_1\rho C_p}$

C_p: specific heat of dry air at constant pressure

ρ: dry air density

Let H_{as} be the sensible anthropogenic heat flux. Then, the additional forcing due to sensible anthropogenic heat flux is

$$F_{as}=\frac{2\Delta t H_{as}}{\Delta \bar{z}_1 \rho C_p \Pi} \quad (6)$$

where Π is Exner function.

The additional forcing due to sensible anthropogenic heat obtained from Eq. (6) is added to source term in Eq. (5) to obtain the improved representation of the bottom layer in the boundary layer scheme.

With similar treatment, latent anthropogenic heat flux, H_{al}, is included in the bottom layer of the moisture equation. The additional forcing due to latent anthropogenic heat flux is

$$F_{al}=\frac{2\Delta t H_{al}}{\Delta \bar{z}_1 \rho L \Pi} \quad (7)$$

where L is latent heat of vaporization.

3.3 Summertime scenarios

Stable and generally non-precipitating week of August (8-14), 2007 was selected for the highly urbanized Osaka City to observe the urban heat island effect. To quantify the urban heat island effect over a long period of time, one-week average of near-surface air temperature was analyzed. Four scenarios were developed, viz.,

(a) Default: WRF only,
(b) AH: WRF with anthropogenic heat (AH),
(c) UCM: WRF with urban canopy model (UCM), and
(d) AH+UCM: WRF using both anthropogenic heat and urban canopy model.

4. Results and discussion

4.1 Near-surface air temperature

The results discussed here are one-week average of near-surface air temperature for each hour of the day (Fig. 5). The three columns in Fig. 5 depict the near-surface air temperature difference of AH, UCM, and AH+UCM scenarios with respect to the default case (refer section 3.3). These near-surface air temperature results are for Osaka City only. From Fig. 5, some important results are discussed here.

In AH-Default case, near-surface air temperature increases prominently in Osaka City from 2000 JST to 0700 JST. The maximum increase over this region is seen at 0700 JST. At daytime, an increase in near-surface air temperature at the high-anthropogenic heat spot in and around Umeda region is generally observed.

In UCM-Default case, near-surface air temperature increases over the entire Osaka City region from 2200 JST to 0600 JST, except over the Osaka Castle area where near-surface air temperature is generally not affected by urban canopy. The maximum increase over this region is seen at 0300-0400 JST. From 0900 JST to 1800 JST, near-surface air temperature slightly decreases, especially in the northern and eastern Osaka City. This localized cooling effect may be attributed to the effect of urban canopy as well as the green spaces like parks and suburban vegetation interspersed in the urban setting of Osaka City.

Table 3 Maximum and average differences in near-surface air temperature for three simulation cases

Cases	Maximum difference (K)	Average difference (K)
AH – Default	0.8	0.2
UCM – Default	2.2	0.7
(AH+UCM)-Default	2.5	0.8

In (AH+UCM)-Default case, using both anthropogenic heat and urban canopy model, prominently high increase in near-surface air temperature is observed from 2100 JST to 0700 JST. Compared to UCM-Default case, localized increase in near-surface air temperature is observed from 0 hour to 0500 JST in and around the high-anthropogenic heat region. From 0900 JST to 1800 JST, the cooling effect of UCM is partly canceled by the introduction of anthropogenic heat.

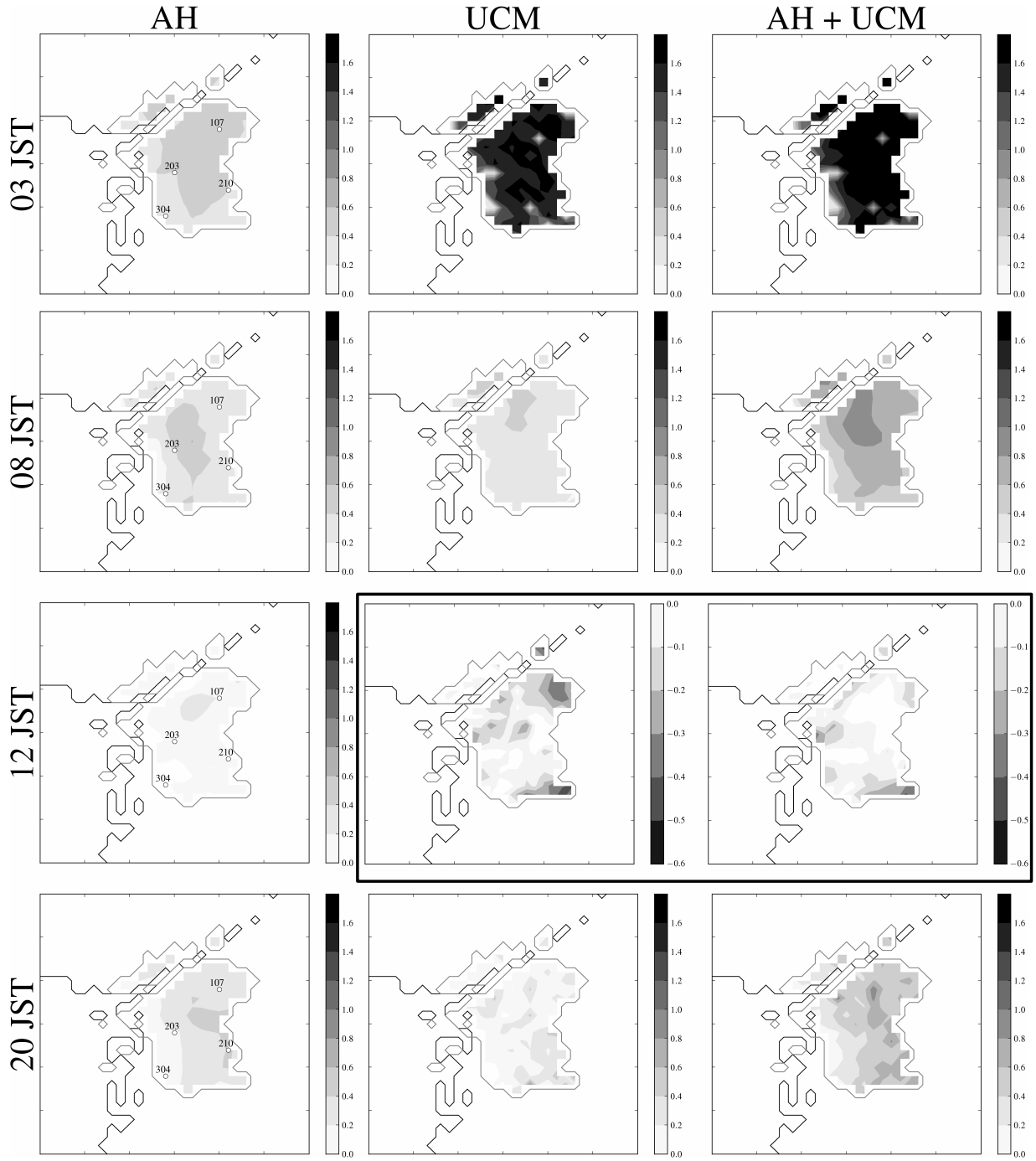

Fig. 5 Time-varying difference plots of the near-surface air temperature differences (deducting the values of the default case from the three other cases) in Osaka City. Only selected hours are shown. UCM and (AH+UCM) cases at 1200 JST have scales different than that of the other cases, and in these two figures, darker shades represent cooling effect mainly due to urban canopy. In the left column, four points are observation stations in Osaka City.

Table 3 shows the largest changes in the near-surface air temperature of the AH, UCM and (AH+UCM) cases with respect to the default case. The UCM case shows a higher contribution to the rise in the air temperature than the AH case. Nevertheless, AH case shows an appreciable

increase in air temperature, especially at nighttime. Overall, using both AH and UCM in WRF, maximum of 2.5 K increase in near-surface air temperature is observed.

Table 4 Observation stations

No.	Name	Latitude	Longitude
107	Kokusetsu-oosaka	34°40'47"N	135°32'07"E
203	Hirao-shougakkou	34°38'27"N	135°28'27"E
210	Setsuyou-chuugakkou	34°37'12"N	135°32'43"E
304	Sanpou	34°35'38"N	135°28'21"E

4.2 Area-averaged time series

To observe the effect of introducing anthropogenic heat and urban canopy effect on the improvement of overall performance and accuracy of WRF model, the simulated area-averaged time series of Osaka City were compared with the area-averaged observed time series at observation points (see Fig. 1 and Table 4). Since the WRF simulation result for each grid in the domain is a volume-averaged value for that grid, the comparison of area-averaged time series seems to be more meaningful in this context. Since we are observing time series for a very fine grid resolution of 1 km, the fine differences arising from local effects and grid structure can adversely affect the comparison with individual stations. In Fig. 6, the area-averaged time series of urban grids in Osaka City are investigated with respect to the observed time series. For the default case, the area-averaged time series plot shows underprediction at nighttime on most of the days. One of the reasons for this underprediction is that the anthropogenic heat generated in the urban region is not well represented in the WRF model. Another reason is that the urban canopy effect is not represented in the default configuration of WRF model. After using anthropogenic heat and urban canopy model in the WRF model, we see an appreciable increase in the nighttime near-surface air temperature on all the days of the week. When compared with the observed data, the simulation of nighttime air temperature is greatly improved by using anthropogenic heat and urban canopy model in all days except at nighttime between August 12 and 13. Between August 8 and 11, the daytime air temperature is underestimated by the WRF model. One of the main causes of this underestimation can be the model not being able to fully reproduce the synoptic conditions prevalent on those days. The model simulation overpredicts air temperature at nighttime only between August 12 and 13, which may have been caused by the model being unable to fully represent the sudden drop in temperature accompanied with an increase in wind speed in Osaka City. Though rest of the days had good results for nighttime air temperature, we recommend a use of a larger domain to nest the 1-km domain so that synoptic and regional scale phenomena may be better included in the boundary conditions.

In contrast, only a relatively small amount of near-surface air temperature increases at nighttime in non-urban grids of Osaka City. This small increase in nighttime temperature in non-urban grids reflects the effect of large number of urban grids surrounding the non-urban grids. In non-urban grids, it must be pointed out that the actual grid points are surrounded, and hence, affected by different types of urban atmosphere in the Osaka City region. Overall, the complex regional setting of Osaka City, in which greenspaces and open spaces are irregularly interspersed in the urban setting, influences the local climate to create complex temperature patterns.

4.3 One-week averaged time series

To ascertain the diurnal average pattern of near-surface air temperature in Osaka City, the one-week time series at different stations were averaged to 24-hour time series. This type of averaging can eliminate the intra-day time scale fluctuations that are inherent in air temperature results [12], and thus a clear diurnal pattern can be observed.

Four stations in Osaka City having observation data (see left column in Fig. 5 and Fig. 1) have been

selected for one-week averaged time series analysis of urban heat island (Fig. 7). The gross error gets reduced when using AH and UCM. This improvement is mainly attributable to the increase in the nighttime near-surface air temperature when using anthropogenic heat and urban canopy.

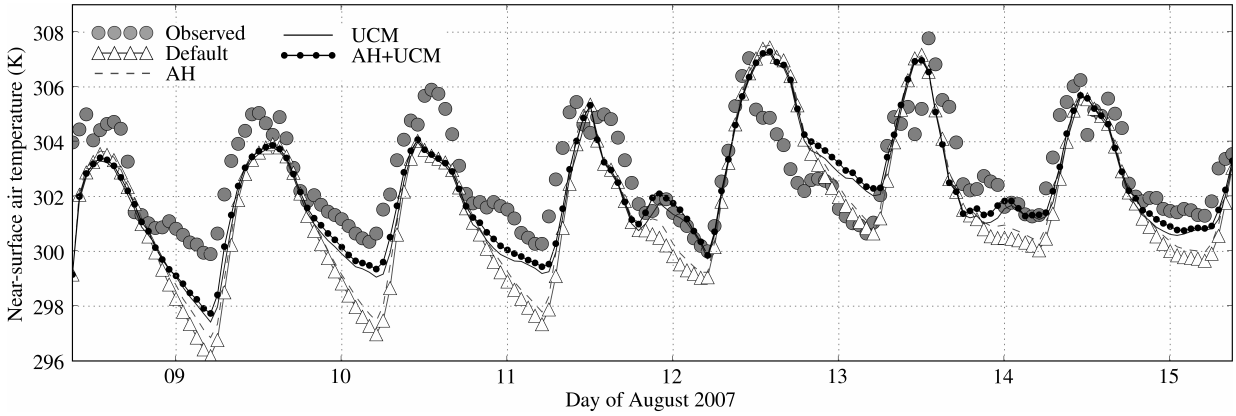

Fig. 6 Area-averaged time series of near-surface air temperature for the different scenarios compared with the observed data in the urban grids of Osaka City.

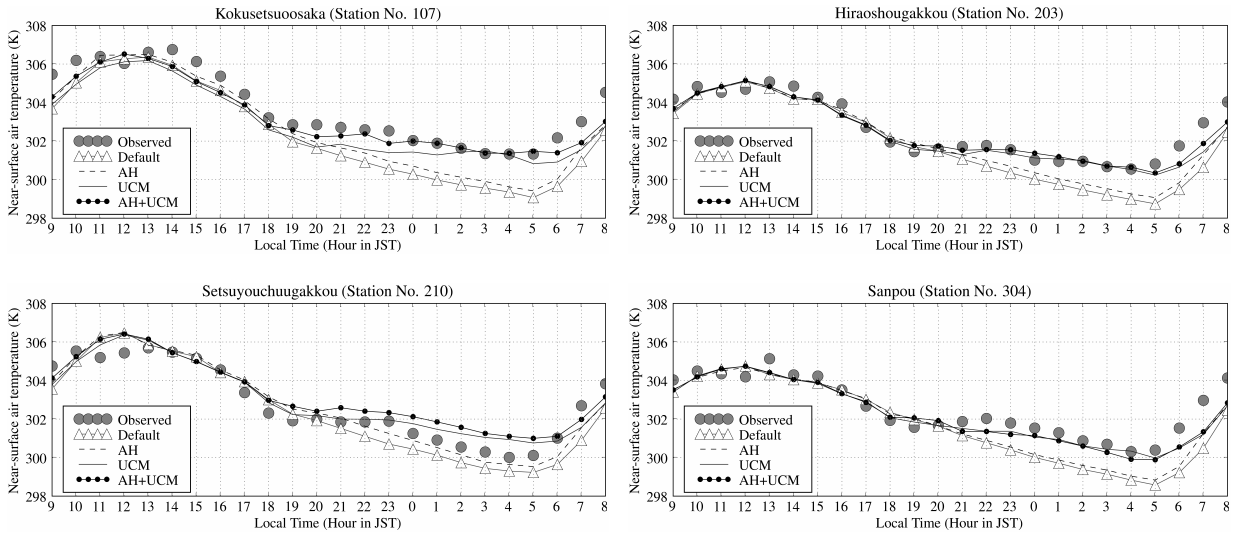

Fig. 7 Time series of near-surface air temperature at four stations in Osaka City (see Fig. 1 and Table 4) for the different scenarios compared with the observed data obtained from Japan Meteorological Agency.

Osaka City has a complex land-use area, and it consists of a combination of highly urban region, Yodo River, greenspaces and open spaces including the Osaka Castle region. Fig. 7 clearly demonstrates that the inclusion of urban canopy effect and anthropogenic heat sources produce better air temperature results at nighttime. On the other hand, in daytime, a small cooling effect is observed due to the inclusion of urban canopy model. This cooling effect seems to have been partially canceled by the effect of anthropogenic heat emission. Thus we can observe a complex effect of anthropogenic heat emission and urban canopy structure on the near-surface air temperature of highly irregular land-use area of Osaka City.

5. Conclusion

WRF model coupled with urban canopy model was modified in the YSU PBL scheme program to include the gridded anthropogenic heat emission data in the potential temperature equation at the first vertical level above the ground. The WRF modeling system was then used to simulate one-week summertime scenarios of 2007 using one-way nesting of 1-km grid domain inside a 3-km grid domain. The scenarios include the default WRF model scenario, WRF coupled with urban canopy model scenario, WRF with anthropogenic heat scenario, and finally WRF coupled with both urban canopy model and anthropogenic heat scenario.

For summertime, area-averaged time series of Osaka City and one-week average of the diurnal variation of near-surface air temperature in observation stations clearly demonstrates the effect of anthropogenic heat, especially at nighttime with a maximum increase of 0.8 K in Osaka City. The urban heat island effect of urban canopy is also confirmed with overall increase in near-surface air temperature at nighttime with maximum increase of 2.2 K, but with a relatively small decrease at daytime. Using both urban canopy model and anthropogenic heat, the nighttime near-surface air temperature is further increased with maximum increase of 2.5 K at regions with high-anthropogenic heat emission, thus simulating a better representation of urban heat. Additionally, in the daytime, the cooling effect of urban canopy is partially canceled out by anthropogenic heat forcing.

Due to the complex land-use pattern consisting of tall buildings, residential area, greenspaces, open spaces, parks, and recreational spots, the diurnal pattern of atmospheric temperature in Osaka City is intricately associated with the urban canopy structure as well as the anthropogenic heat emitted from urban sources. Thus, using WRF model, we obtain an average increase of near-surface air temperature of 0.2 K when anthropogenic heat is considered, 0.7 K when urban canopy is considered, and 0.8 K when both anthropogenic heat and urban canopy structure are taken into account.

References

1) S. Grimmond: The Geographical Journal, **173** (1), 83 (2007).
2) H. Kusaka and H. Hayami: JSME International Journal Series B, **49 (**1), 72 (2006).
3) H. Kusaka and F. Kimura: J. Meteorol. Soc. Jpn., **82**, 67 (2004).
4) H. Kusaka and F. Kimura: J. Appl. Meteorol., **43**, 1899 (2004).
5) H. Kondo, T. Tokairin and Y. Kikegawa: J. Wind Eng. Ind. Aerodyn., **96** (10-11), 1655 (2008).
6) H. Fan and D. J. Sailor: Atmos. Environ., **39** (1), 73 (2005).
7) C.-Y. Lin, F. Chen, J.C. Huang, W.-C. Chen, Y.-A. Liou, W.-N. Chen and S.-C. Liu: Atmos. Environ., **42** (22), 5635 (2008).
8) W. Skamarock, J. Klemp, J. Dudhia, D. Gill, D. Barker, W. Wang and J. Powers: "A description of the Advanced Research WRF Version 2," NCAR Technical note NCAR/TN-468+STR, (2005).
9) H. Kusaka, H. Kondo, Y. Kikegawa and F. Kimura: Boundary Layer Meteorol., **101** (3), 329 (2001).
10) D. Narumi, F. Otani, A. Kondo, Y. Shimoda and M. Mizuno: J. Archit. Plann. Environ. Eng., 562, 97 (2002). (in Japanese).
11) S.-Y. Hong, Y. Noh and J. Dudhia: Mon. Weather Rev., **134** (9), 2318 (2006).
12) K. L. Shrestha, A. Kondo, A. Kaga and Y. Inoue: Proc. 16th International Conference on Modelling, Monitoring and Management of Air Pollution, (ed. by C. A. Brebbia and J.W.S. Longhurst, Skiathos, Greece, September 2008), pp. 429-438, WIT Press, UK (2008).